Wetting and layering transitions in liquid crystals

A. M. Somoza and L. Mederos
Instituto de Ciencia de Materiales, Consejo Superior de Investigaciones Científicas, Cantoblanco, Madrid E-28049, Spain

D. E. Sullivan
Department of Physics and Guelph-Waterloo Program for Graduate Work in Physics, University of Guelph, Guelph, Ontario, Canada N1G 2W1

(Received 20 April 1995)

Interfacial structure in the isotropic phase of a liquid-crystalline material near a wall is studied by a mean-field density-functional theory. With increasing strength of the wall anchoring potential, the theory predicts a first-order transition from incomplete to complete wetting by the smectic-A phase at bulk isotropic-smectic coexistence, with an associated prewetting transition occurring away from bulk coexistence. The incomplete wetting case is accompanied by a small number (between 0 and 2) of discrete layer transitions, while an infinite number of such transitions occurs at complete wetting. An analysis of the underlying physical mechanisms for layer transitions reveals that these transitions tend to disappear as the system is moved both sufficiently close to and sufficiently far from the bulk isotropic–nematic–smectic-A triple point by varying the model coupling parameters. These results reconcile findings from previous theories and experiments.

PACS number(s): 61.30.Cz, 64.70.Md, 68.45.Gd

I. INTRODUCTION

Phase transitions at interfaces of liquid crystals is a subject of ongoing interest. One reason for this is the fact that these transitions involve the interplay of several phenomena, such as wetting, roughening, and orientational ordering [1,2]. Interfaces of smectic liquid-crystalline phases add further complexity, associated with positional ordering, which can give rise to a variety of layering phenomena. Several x-ray reflectivity experiments [3–5] have studied the development of smectic-A (denoted A) ordering at interfaces of liquids which are isotropic (I) in bulk, on approaching the bulk first-order I-A transition temperature T_{IA} from higher temperatures. These works have examined either the "free," i.e., liquid-vapor interface [3,4], or the interface between the liquid and a solid substrate [5]. A recent generalization of the latter study has been applied to interfaces within finite-sized pores [6]. These experiments have revealed the occurrence of discrete layering transitions, i.e., discontinuous increases in the number of spontaneously formed smectic layers, as the systems are cooled toward T_{IA}. This can be interpreted as layer-by-layer wetting of the interface by the A phase. Layer transitions have also been observed during compression of insoluble films of liquid crystals spread on a water-air interface [7,8]. Related phenomena, layer-*thinning* transitions, have recently been seen in temperature scanning studies of free-standing liquid-crystal films [9].

The above-cited studies of smectic ordering at semi-infinite interfaces [3–5] have indicated that discrete-layer growth terminates after a finite number of smectic layers, less than or equal to six, which implies that wetting by the A phase is incomplete. All of these studies have examined compounds of the homologous cyanobiphenyl series nCB, where n denotes the length of the alkane tail of the molecules. The smectic film growth has been shown to become progressively more continuous in nature, i.e., with fewer discrete transitions, as n decreases from 12 to 10. Below a value of n between 9 and 10, the bulk isotropic phase undergoes a direct transition to the nematic (N) rather than the A phase. Earlier studies [10,11] of the compounds 5CB and 8CB have shown that in these cases the N phase completely wets the free surface.

Previous studies of smectic layering at interfaces using mean-field theory have predicted results at variance with each other and with the experimental results described above [12–14]. Both Ref. [12] and Ref. [13] modeled the free interface by an external anchoring potential of adjustable strength. The work in Ref. [13], based on a generalization of McMillan's [15] theory for bulk transitions to the A phase, predicted incomplete smectic wetting from the bulk isotropic phase, accompanied by up to two discontinuous layer transitions. These qualitative results were found to be independent of the strength of the anchoring potential. In contrast, using a lattice model, Ref. [12] predicted that a first-order transition from incomplete to complete smectic wetting occurred with increasing strength of the anchoring potential. No smectic layering at all was found in the nonwetting case, while the complete-wetting case was accompanied by an infinite number of layer transitions. The use of an external potential more closely models the physics at the interface between a liquid and an inert solid substrate rather than at a free interface. A density-functional theory more appropriate to the free interface, representing this by the true diffuse interface between coexisting liquid and vapor phases, was considered by two of the present authors in

Ref. [14]. A weak degree of smectic-A ordering at the interface was found, consistent with incomplete wetting, but no discrete transitions in the number of smectic layers were detected.

In this paper we describe results obtained from a generalization of the density-functional theory in Ref. [14], which partially reconciles the previous theoretical findings. (A preliminary report of this study appeared earlier [16].) Here we have extended the theory to the case of an interface between a bulk isotropic liquid and a rigid substrate or wall, representing the latter by an external potential similar to that used in Refs. [12,13]. As in Ref. [12], we find that there is a first-order wetting transition with increasing strength of the wall potential, where the adsorbed smectic film in the complete-wetting case grows via an infinite sequence of discrete-layer transitions. However, we also find that there are a small, variable number (between 0 and 2) of layer transitions in the case of incomplete smectic wetting, which occurs for sufficiently weak strength of the wall potential. This is similar to the results described in Ref. [13], although the latter found no evidence of a wetting transition. Due to the first-order nature of the wetting transition reported here, it is accompanied by a prewetting transition [17] which extends away from bulk I-A coexistence, at which the adsorbed smectic film can increase in thickness by an arbitrary number of layers. The occurrence of a prewetting transition was apparently overlooked in Ref. [12], perhaps because it is confined to a very narrow domain near bulk coexistence.

After briefly reviewing the theory and describing its current extension in Sec. II, Sec. III presents the full details of our analysis and results. The results are first summarized by means of surface phase diagrams. These are deduced by examining the changes in interfacial structure during layer transitions, illustrated by profiles of the number density and orientational order parameter near the wall. Determining the phase boundaries of the layer transitions and prewetting transition requires a precise analysis of the interfacial tension γ, in particular its behavior as a function of the thickness of the adsorbed smectic film. Finding this variation is facilitated by the existence of many metastable interfacial structures corresponding to films with different numbers of smectic layers. In Sec. IV we present qualitative arguments based on two complementary physical mechanisms, which account for many of the features exhibited by our results. Of most significance, we show that layer transitions occur only within a narrow range of values of the coupling constants of the model, which in turn indicates that the transitions tend to disappear both very near and far from the bulk I-N-A triple point. The feature that layer transitions disappear on approaching the I-N-A triple point agrees, of course, with the experimental observations described earlier, while the more general finding is shown to be consistent with theoretical results obtained in Refs. [12,13]. The paper concludes with a discussion in Sec. V.

II. THEORY

The present theory [14,18] is based on a classical density-functional approximation to the grand canonical potential Ω of an inhomogeneous molecular fluid. The molecules are assumed to interact pairwise via a hard-spheroid repulsive core potential, with major and minor diameters $\sigma_{\|}$ and $\sigma_{\perp}$, respectively, and a long-range anisotropic attractive potential denoted $V_A(12)$. Here i (i=1,2) stands for the position $\mathbf{r}_i$ and Euler angles ω_i specifying the orientation of molecule i. Explicitly, $V_A(12)$ is given by

$$V_A(12) = \epsilon_1 V_1(r_{12}) + \epsilon_2 V_2(r_{12}) P_2(\cos\theta_{12}) + \epsilon_3 V_3(r_{12})[P_2(\cos\theta_1') + P_2(\cos\theta_2')], \quad (1)$$

where $r_{12} \equiv |\mathbf{r}_{12}|$ is the intermolecular separation, θ_{12} is the angle between the symmetry axes of molecules 1 and 2, $\theta_i'(i = 1, 2)$ is the angle between the intermolecular vector $\mathbf{r}_{12}$ and the symmetry axis of molecule i, and P_2 denotes the second Legendre polynomial. The dimensionless functions $V_n(r)$ are given by Lennard-Jones potentials truncated inside the molecular core [see Eq. (3) in Ref. [14], where the $V_n(r)$ include the coupling strengths ϵ_n shown explicitly in Eq. (1) above]. The term $\epsilon_1 V_1(r)$ describes isotropic attractive interactions responsible for liquid-vapor phase separation. The second term $\epsilon_2 V_2(r) P_2(\cos\theta)$ is a Maier-Saupe-type [19] interaction which promotes nematic ordering, while the third term, with coupling strength ϵ_3, provides symmetry breaking between different parallel orientations of molecular pairs and thus promotes smectic ordering.

The contribution of the long-range interaction $V_A(12)$ to the grand potential is treated by a standard mean-field approximation. The hard-core contribution to Ω is evaluated by a "weighted-density" technique [18,20]. Here the anisotropic core shape is taken into account by means of a scaling argument which assumes that the molecular symmetry axes are all perfectly aligned in the z direction, normal to the interface, although elsewhere in Ω (i.e., in the ideal-gas and mean-field contributions) an arbitrary degree of orientational ordering is allowed. Further discussion of this scheme, including its obvious limitations, is given in Refs. [14,18].

The presence of the wall is accounted for by two modifications of the grand potential Ω given in Ref. [14]. First, the wall confines the fluid to the half space $z \geq 0$. This simply amounts to setting $\rho(z,\theta) = 0$ for $z < 0$, where $\rho(z,\theta)$ is the single-particle probability density, a function of normal distance z and the angle θ between the molecular axis and the z axis. The wall also interacts with molecules at $z \geq 0$ through a long-range anchoring potential,

$$V_{\mathrm{ex}}(z,\theta) = -\frac{\epsilon_w P_2(\cos\theta)}{(1 + z/\sigma)^3}. \quad (2)$$

Here $\sigma = (\sigma_{\|}\sigma_{\perp}^2)^{1/3}$ is a mean hard-core diameter. Apart from its range, this is the same angular coupling used in Refs. [12,13]. This contributes an additional term to the grand potential per unit area A beyond that considered in Ref. [14], namely,

$$\frac{\Omega_{ex}}{A} = 2\pi \int_0^\infty dz \int_0^{2\pi} \sin\theta d\theta \rho(z,\theta) V_{ex}(z,\theta)$$

$$= -\epsilon_w \int_0^\infty dz \frac{\rho(z)\eta(z)}{(1+z/\sigma)^3}, \quad (3)$$

where $\rho(z)$ is the number density and

$$\eta(z) = 2\pi \int_0^{2\pi} \sin\theta d\theta \frac{\rho(z,\theta)}{\rho(z)} P_2(\cos\theta) \quad (4)$$

is the orientational order parameter [denoted $\bar{\eta}(z)$ in Ref. [14]]. Considering Ω as a functional of $\rho(z)$ and $\eta(z)$, the equilibrium structure is obtained by minimization of Ω with respect to both of these functions. As in Ref. [14], space is discretized in the z direction with step size Δz, and the minimization with respect to density and order parameter at every mesh point is performed using the conjugate gradient algorithm. The mesh is extended up to a maximum distance z_{max} beyond which both $\rho(z)$ and $\eta(z)$ are assumed to have constant values equal to those in the bulk I phase. We have used values of z_{max} between 10σ and 60σ, depending on the wetting state of the surface phase. With regard to the mesh size, we have used $\Delta z = 0.05\sigma$ in all our calculations. We have checked that smaller Δz values do not change the qualitative predictions of our theory but significantly increase the computational effort. For consistency, the properties of the bulk I and A phases were calculated using the same numerical procedure, employing periodic boundary conditions in the z direction.

III. RESULTS

A. Surface phase diagram

This model produces a rich variety of surface phase behavior, depending on the values of the interaction parameters. Henceforth, the isotropic interaction strength ϵ_1 and the mean core diameter σ will be used as the units of energy and distance, respectively. In the following results, the major core diameter $\sigma_{||}$ has been fixed at the value 1.8, which has been found in previous work [18] to favor formation of the bulk A phase over a considerable range of temperature and density. The relative stability of the bulk I, N, and A phases then depends on the two remaining parameters ϵ_2 and ϵ_3 characterizing the potential $V_A(12)$, while the surface behavior depends additionally on the wall strength ϵ_w. We have centered our attention on two particular cases obtained under conditions of fixed temperature, ϵ_2 and bulk isotropic density ρ_b.

(A) $T = 0.31$ (in units of ϵ_1/k_b), $\epsilon_2 = 0.43$ (in units of ϵ_1) and density $\rho_b = 0.55$ (in units of σ^{-3}). Under these conditions, we find that the bulk fluid undergoes a direct I-A transition at $\epsilon_3 = -0.656\,62 \equiv \epsilon_3^*$.

(B) $T = 0.32$, $\epsilon_2 = 0.2$, and $\rho_b = 0.50$. In this case, $\epsilon_3^* = -1.027\,34$.

Our principal results for cases (A) and (B) are summarized in the qualitative surface phase diagrams shown in Fig. 1(a) and Fig. 1(b), respectively. This figure plots the boundaries of the surface phase transitions under variations of the coupling parameters ϵ_w and $\Delta\epsilon_3 \equiv \epsilon_3 - \epsilon_3^*$, where the latter measures distance from the bulk I-A boundary. In order to accommodate all of the important results, the scales of both axes in Fig. 1 are only schematic. The numerical values of the coordinates at several key points in the figure are listed in Table I.

The figure shows the prewetting transition (bold line) and a number of individual layer transition lines which terminate at surface critical points. The layer transitions on the low-ϵ_w side of the prewetting line, along with their associated critical points, are explicitly labeled. (How we count the number of adsorbed smectic layers will be described below in Sec. III B.) For case (A), it is seen that the transitions from zero to one and from one to two layers start on the vertical axis, $\Delta\epsilon_3 = 0$, below the prewetting line. Hence, in this range of the wall strength ϵ_w, the interface can exhibit up to two layer transitions at bulk coexistence, and the interface remains incompletely wet by smectic A. One other layer transition, from two to three layers, branches off the low-ϵ_w side of the prewetting line at $\Delta\epsilon_3 > 0$, away from bulk coexistence. As is indicated by the values of $\Delta\epsilon_3$ at the layer critical

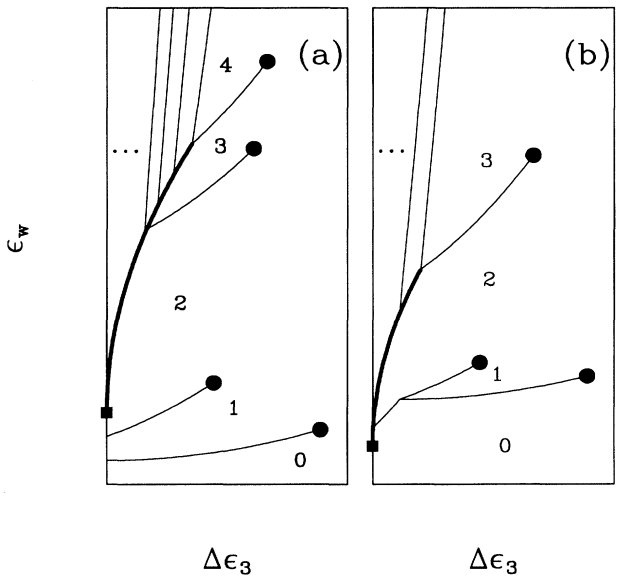

FIG. 1. (a) Theoretical surface phase diagram in the $(\epsilon_w, \Delta\epsilon_3)$ plane for case (A), showing individual layer transitions (thin lines) and the prewetting line (bold line). The number of smectic layers in different regions are indicated. The filled square on the vertical axis represents the wetting transition at bulk coexistence, while the filled circles are layer critical points. The scales on both axes are only schematic: in particular, the relative ordering vs ϵ_w of the (0-1), (1-2) critical points and the (3-4-5) triple point is not shown correctly (see Table I). (b) Same as (a) for case (B).

TABLE I. $(\epsilon_w, \Delta\epsilon_3)$ values of some key points in the surface phase diagrams shown in Fig. 1. A and B correspond to Figs. 1(a) and 1(b), respectively. The number of smectic layers of the different coexisting structures is indicated between parentheses. The subindex "coex" corresponds to bulk *I-A* coexistence while "crit" corresponds to a surface critical point. The other entries labeled by three layer numbers refer to surface triple points.

	ϵ_w	$\Delta\epsilon_3$
A: $(0\text{-}1)_{\text{coex}}$	0.40	0.000
A: $(1\text{-}2)_{\text{coex}}$	0.45	0.000
A: $(2\text{-}\infty)_{\text{coex}}$	0.48	0.000
A: $(0\text{-}1)_{\text{crit}}$	0.68	0.277
A: $(1\text{-}2)_{\text{crit}}$	0.63	0.043
A: $(2\text{-}3)_{\text{crit}}$	1.25	0.050
A: $(3\text{-}4)_{\text{crit}}$	3.42	0.053
A: (3-4-5)	0.51	4.5×10^{-4}
B: $(0\text{-}\infty)_{\text{coex}}$	0.38	0.000
B: (0-1-2)	0.39	2.9×10^{-3}
B: $(0\text{-}1)_{\text{crit}}$	0.94	0.510
B: $(1\text{-}2)_{\text{crit}}$	0.63	0.052
B: $(2\text{-}3)_{\text{crit}}$	1.42	0.055
B: (2-3-4)	0.40	7.6×10^{-4}

points given in Table I, with the exception of the 0-1 critical point, all these layer transitions occur very close to the bulk *I-A* phase boundary. An infinite number of layer transitions branches off from the high-ϵ_w side of the prewetting line. Due to the close proximity of the higher-layer transition lines to the vertical ϵ_w axis and to limitations imposed by the finite values of $z_{\max}$ allowed in our calculations, the precise locations of these transitions and their critical points have not been determined. Nonetheless, the evidence supporting an infinite number of layer transitions and hence complete wetting by the *A* phase is quite strong, as will be described in detail below in Sec. III C. The prewetting line is thus the locus of coexistence between films of two or three layers in thickness and films of thickness greater than four layers. On a finer scale of resolution than is used in Fig. 1, one would see that the prewetting line is really composed of an infinite set of smooth curves between successive surface triple points, at which small discontinuities in the slope $d\epsilon_w/d\epsilon_3$ occur.

A feature of the present results is that the prewetting line does not terminate away from bulk coexistence at a (prewetting) critical point, as is normally the case [21]. Instead, in case (A), it terminates at the surface triple point forming the junction of the 3-4 and 4-5 layer transition lines, which eventually terminate at their own critical points. Note by comparison with Table I that the extent of the prewetting line in the ϵ_w direction is greatly exaggerated in Fig. 1. At its opposite limit, the prewetting line approaches the ϵ_w axis with an infinite value of the slope $d\epsilon_w/d\epsilon_3$. While we cannot extend our numerical calculations all the way to this limit, due to the infinite thickness of the resulting wetting layer at bulk coexistence, the occurrence of an infinite slope as $\Delta\epsilon_3 \to 0$ can be proven by an analytical argument analogous to that described in Ref. [22], based on the behavior of Ω in this limit.

For case (B), the range of stability of the zero-layer surface phase has increased relative to the one- and two-layer films. However, the wetting transition is reached at a smaller value of ϵ_w. As a consequence, at the prewetting transition near bulk coexistence, a thin film without smectic structure coexists with a thick film, which is similar to the behavior found in Ref. [12]. A new feature, compared with case (A), is the appearance of a 0-1-2 layer triple point, while the end of the prewetting line now corresponds to the 2-3-4 layer triple point. The rest of the phase diagram is qualitatively similar to the previous case. Explanation of the differences between cases (A) and (B) will be given in Sec. III C.

Figure 2 shows, for case (A), the same surface phase diagram of Fig. 1(a) plotted in the η_{int} vs $\Delta\epsilon_3$ plane. Here η_{int} is the net orientational order parameter integrated over the liquid half space $z \geq 0$, i.e.,

$$\eta_{\text{int}} = \int_0^\infty dz\eta(z), \tag{5}$$

which we can consider as a measure of the thickness of the adsorbed smectic film. The various shaded areas are the coexistence regions associated with the layer transitions. This figure is plotted quantitatively but, on this scale, we cannot see the prewetting coexistence curve, which would include an infinite sequence of triple (and perhaps higher-order multiphase) points. The start of this curve is indicated by the square symbol on the vertical axis. The other side of the prewetting curve would diverge on approaching this axis, due to complete wetting at bulk coexistence.

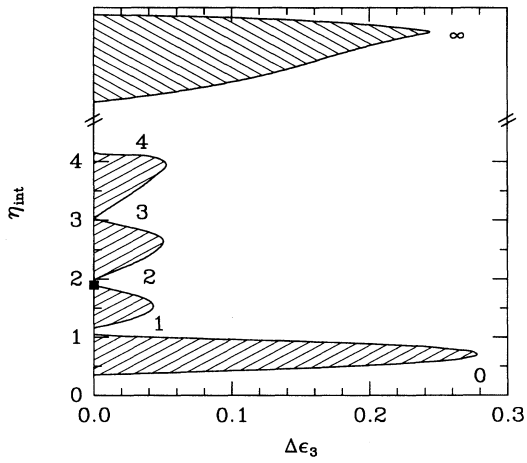

FIG. 2. Same surface phase diagram as Fig. 1(a) in the $(\eta_{\text{int}}, \Delta\epsilon_3)$ plane. The prewetting line is not seen on these scales. The shaded areas are the layer-transition coexistence regions.

Figure 2 also shows the layer transition which occurs infinitely far away from the wall (note the cut in the vertical axis). Two particular features to note about this transition are that it terminates away from bulk coexistence and that the termination point is a *bulk tricritical* rather than a surface critical point, yielding the cusp at the apex of the coexistence region. These features can be derived on assuming that, for $\eta_{\rm int} \to \infty$ and $\Delta\epsilon_3 > 0$, the position z_0 of the interface between the smectic film and bulk isotropic liquid diverges in such a way that the wall potential $V_{\rm ex} \approx -(\epsilon_w/{z_0}^3)P_2(\cos\theta)$ approaches a nonzero constant value. Since the gradient of this potential with respect to z at z_0 vanishes faster than $V_{\rm ex}$ itself as $z_0 \to \infty$, one can consider the fluid in this region to be in a uniform external field. The layer transition can then be described as the addition of a single layer to the bulk smectic phase which coexists with an "isotropic" liquid in the presence of this field, a process which merely shifts the position of the interface without affecting either its shape or the value of the interfacial tension. It should be noted that the bulk "isotropic" phase in this case has nonvanishing orientational order due to the external field, and thus is more properly termed a paranematic phase [23,24]. The jump in $\eta_{\rm int}$ is then given simply by $\Delta\eta_{\rm int} = \lambda(\eta_{\rm sm} - \eta_p)$, where λ is the bulk smectic period and $\eta_{\rm sm}$, η_p are the order parameters in the coexisting smectic and paranematic phases, respectively. Thus it is only necessary to obtain solutions of the theory for two-phase coexistence in a bulk fluid in the presence of a uniform external potential $V_{\rm ex}(\theta)$ at a given value of $\Delta\epsilon_3$. This calculation yields the data for $\Delta\eta_{\rm int}$ at the infinite-layer transition plotted in Fig. 2. In the particular case of $\Delta\epsilon_3 = 0$, $\eta_p = 0$ and the values of $\eta_{\rm sm}$ and λ are just those at bulk I-A coexistence in the absence of an external field.

B. Interfacial structure and free energy

The results in Figs. 1 and 2 are based on the behavior of the interfacial structure and thermodynamics. Generally, under parameter conditions which favor layering, one finds several different simultaneous solutions of the theory, which represent interfacial structures exhibiting different numbers of smectic layers. As usual, the thermodynamically stable structure corresponds to that solution having the smallest value of the surface excess grand potential, i.e., interfacial tension γ. (See [14] for the evaluation of γ in the present theory.) Layer transitions are located where two solutions have equal values of γ. Examples of such simultaneous solutions for the first two layer transitions at bulk I-A coexistence (i.e., for $\Delta\epsilon_3 = 0$) in case (A) are given in Fig. 3. Figure 3(a) shows the number density and order-parameter profiles of the two coexisting surface structures, having equal values of γ, at the 0-1 transition. It is seen that the density of the zero-layer phase increases over a short distance from its contact value at $z = 0$, and thereafter is mostly featureless. This is characteristic of a *partial-drying* state. In contrast, the one-layer profile exhibits a large density peak near $z = 0$, as well as progressively weaker

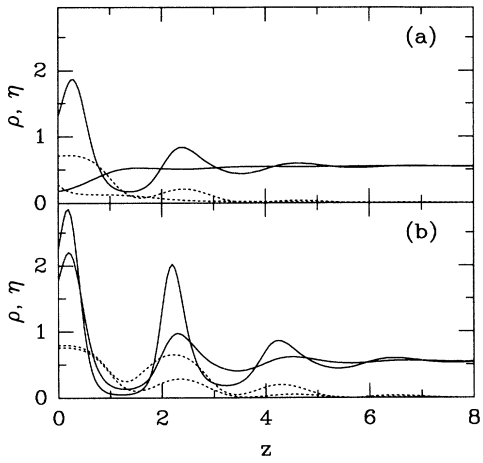

FIG. 3. (a) Density (continuous lines) and order-parameter (dotted lines) profiles of coexisting surface structures at the transition between zero and one smectic layer in case (A) at bulk coexistence. (b) Same as (a) but for the 1-2 layer transition.

peaks representing partial filling of the second and third layers. The spacing between successive peaks is approximately $\sigma_{\|}$. Related features are seen in the behavior of the order parameter. Figure 3(b) shows the corresponding structural changes at the 1-2 transition, which takes place at a slightly larger value of ϵ_w. In this case, the largest changes in both $\rho(z)$ and $\eta(z)$ occur at their respective second peaks away from the origin, but increases in both functions also occur at the first and third peaks. The relative change in $\eta(z)$ near the first peak is rather small, indicating that the orientational ordering in the first layer is nearly saturated, which suggests regarding $\eta(z)$ as the more appropriate order parameter for indicating layer transitions. We have found that a good "thumb rule" for deciding whether a layer transition has occurred is based on comparing the maximum value $\eta_{\rm max}$ of $\eta(z)$ in a layer with the value $\eta_{\rm coex} \approx 0.42$ predicted by the Maier-Saupe [19] model for *nematic-isotropic* coexistence. If $\eta_{\rm max} > \eta_{\rm coex}$, then the layer is smectic, and otherwise it corresponds to a structured liquid.

In general, the structural changes at the layer transitions in case (B) are similar to those described above.

The determination of the layer transition points, by comparing the values of γ for the separate zero-, one- and two-layer structures as functions of ϵ_w, are illustrated in Fig. 4. Figure 4(a) applies to case (A) at bulk coexistence. [The profiles shown in Fig. 3 correspond to the coexisting structures at the two crossing points in Fig. 4(a).] Figure 4(b) shows analogous plots for case (B) near bulk coexistence ($\Delta\epsilon_3 = 1.4 \times 10^{-4}$). In the latter case, one notes that the one-layer structure is always metastable with respect to the other profiles, which has been indicated by a dashed line. Figure 5 displays the corresponding variations of the integrated order parameter $\eta_{\rm int}$ vs ϵ_w. The vertical solid lines indicate the layer

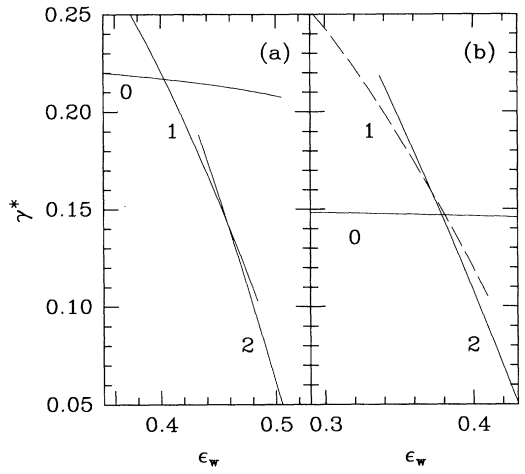

FIG. 4. (a) Reduced surface tension, $\gamma^* = \gamma\sigma^2/k_BT$, versus wall potential strength ϵ_w for zero-, one-, and two-smectic-layer structures in case (A) at bulk coexistence. The layer transitions take place at the intersecting points. (b) Same as (a) for case (B) near bulk coexistence. The one-layer structure is always metastable under these conditions (indicated by a dashed line).

transitions while the vertical dotted lines denote the wetting or prewetting transitions. The occurrence of a significant range of ϵ_w over which the distinct structures are metastable is clearly seen in the latter two figures. Figure 5(a) applies to case (A) at bulk I-A coexistence, and corresponds to both Fig. 4(a) and Fig. 3. Figure 5(b) describes case (B) slightly away from bulk coexistence, and corresponds to Fig. 4(b). The dashed line again indicates the metastable character of the one-layer structure. It is interesting to note the proximity between the 0-2 layer transition and the prewetting one. Closer to bulk coexistence, the 0-2 transition is preempted by the wetting transition, as shown in Fig. 1(b).

Figure 5(c) pertains to the new case $T = 0.31$, $\epsilon_2 = 0.43$, and $\rho_b = 0.70$ at bulk I-A coexistence [i.e., similar to case (A) but at a higher bulk density]. In this case, we obtain a smooth curve of $\Delta\eta_{\rm int}$ vs ϵ_w until the wetting transition, and all indications of the 0-1 and 1-2 transitions have disappeared. In the metastable region, the 2-3 transition has also disappeared, although a shoulder remains as a signature of associated pretransitional effects. We will come back to this point in Sec. IV.

Similar features to those shown in Fig. 5 are exhibited by the coverage, $\Gamma = \int_0^\infty dz\rho(z)$.

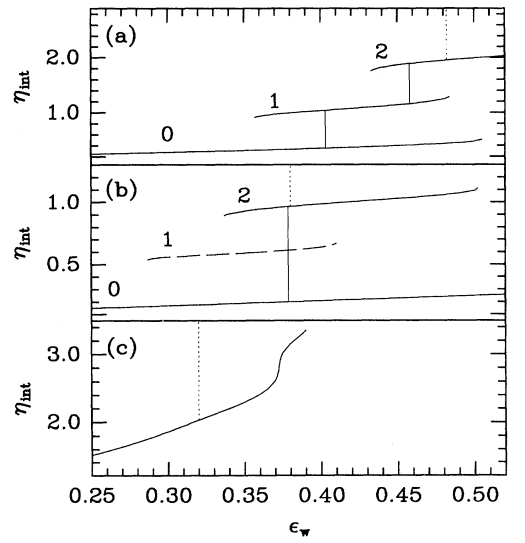

FIG. 5. (a) Integrated order parameter, $\eta_{\rm int}$ versus wall potential strength ϵ_w for zero-, one-, and two-smectic-layer structures [case (A)]. The solid vertical lines are at the layer transitions [corresponding to the intersecting points in Fig. 4(a)]. The vertical dotted line represents the wetting transition. (b) Same as (a) for case (B). (c) Same as (a) for $T = 0.31$, $\epsilon_2 = 0.43$, and $\rho_b = 0.7$.

C. Wetting and prewetting

To determine whether or not the A phase completely wets the interface, and whether in the former case the wetting film grows via an infinite sequence of first-order layer transitions, strictly requires evaluating the behavior of very thick adsorbed films. In practice, we are limited numerically to studying films no greater than about 20 smectic layers in thickness. However, we believe that the following results in support of our conclusions in Fig. 1 are compelling.

As already noted, we can generally find numerous metastable solutions of the theory. Examples of metastable "thick-film" structures in case (A) are given in Figs. 6(a) and 6(b), which show $\rho(z)$ and $\eta(z)$ at $\Delta\epsilon_3 = 0$ for films of thicknesses 20 and 22 layers, respectively. These profiles are the final converged results

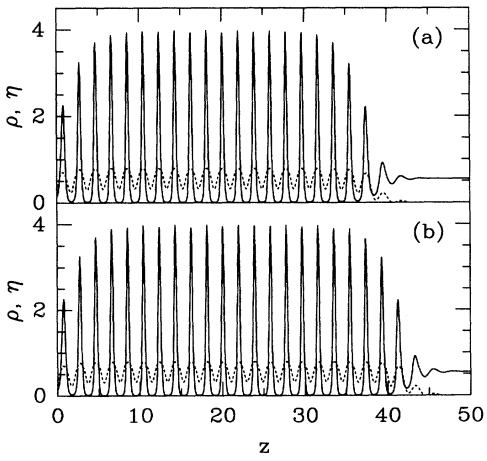

FIG. 6. Density (continuous lines) and order-parameter (dotted lines) profiles at bulk coexistence for $\epsilon_w = 0$ in case (A). (a) corresponds to a thick smectic film of 20 layers while (b) contains 22 layers.

from the numerical minimization of Ω, obtained by initializing the calculation with trial profiles containing the same numbers of layers, 20 and 22, respectively, indicating that both sets of profiles represent relative minima of the interfacial tension γ. In this example, the wall coupling strength is $\epsilon_w = 0$, well *below* the values for the first two layer transitions and the wetting transition (see Table I). The surface tensions of these structures are $\gamma_{20} = 0.876\,08$ and $\gamma_{22} = 0.876\,10$, to be compared with that of the zero-layer structure, $\gamma_0 = 0.228\,75$ (all in units of k_BT/σ^2). The fact that the numerical algorithm does not "flow" toward the absolute interfacial tension minimum at zero layers clearly suggests the presence of significant metastability barriers between structures differing in the number of smectic layers. Furthermore, these results suggest that such metastability barriers persist in films of arbitrarily large thickness, for sufficiently small $\Delta\epsilon_3$, which supports the conclusion that such films grow via an infinite sequence of layer transitions. This is consistent with the mean-field nature of the theory, which precludes thermal roughening effects that could eliminate high-n layer transitions [21,25].

By superimposing the profiles in Figs. 6(a) and 6(b), one sees that their shapes near both the wall at $z = 0$ and the outer film-bulk interface are virtually identical. This supports our earlier method of analyzing the infinite-layer transition.

Strong evidence for the occurrence of a prewetting (and, by implication, a wetting) transition can be obtained by examining somewhat thinner films. This is illustrated in Fig. 7, which plots γ vs wetting-layer thickness (as measured by $\eta_{\rm int}$) for both cases (A) and (B), for some pairs of values of $(\epsilon_w, \Delta\epsilon_3)$ which approximately lie along the prewetting curves. The discrete points on each curve show the final converged values of γ for structures containing from zero to 14 layers. All of these are

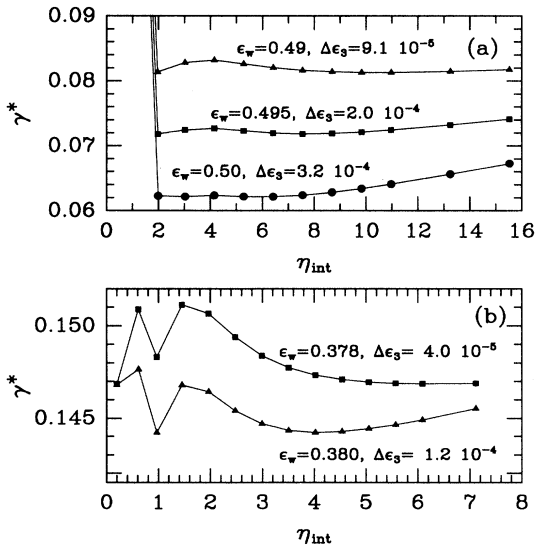

FIG. 7. (a) Curves of surface tension, $\gamma^* = \gamma\sigma^2/k_BT$, versus integrated order parameter $\eta_{\rm int}$ on approaching the prewetting critical point, for the indicated values of ϵ_w and $\Delta\epsilon_3$ in case (A). (b) Same as (a) for case (B).

local minima of the interfacial tension, with the majority corresponding to metastable states. The smooth lines connecting the points are only a guide to the eye, but are similar to curves of interfacial tension vs wetting-layer thickness generated in previous models where the wetting-layer thickness is a continuous order parameter [17]. Here these lines are presumed to be envelopes through the local minima of more detailed interfacial tension curves exhibiting alternating minima and maxima, the latter representing the metastability barriers [26].

Figure 7(a) pertains to case (A). For the range of the parameters $(\epsilon_w, \Delta\epsilon_3)$ considered, the values of γ for the metastable zero-layer structure lie outside the scale, while the one-layer state is not a local free-energy minimum under these conditions. From top to bottom, the curves in Fig. 7(a) correspond to increasing values of both ϵ_w and $\Delta\epsilon_3$ and thus characterize points along the prewetting curve in Fig. 1(a) and Fig. 2 at increasing distance from the wetting transition at bulk coexistence. Each curve exhibits two global minima with approximately equal values of γ, describing coexistence of "thin" and "thick" smectic films. In the top two curves, the thin film contains two smectic layers, while the thick film varies from nine to seven layers. In the bottom curve, the coexisting films contain three and six layers. Beyond the thick-film minima, γ increases approximately linearly with increasing thickness, as expected away from bulk I-A coexistence [17]. The behavior of the points near the global minima clearly demonstrates the possibility of producing surface triple points where three structures coexist, two of which differ by one smectic layer. A special case would be the triple point at the coexistence of three-, four-, and five-layer films, which terminates the prewetting curve, as discussed earlier.

Several different features are shown in Fig. 7(b), which corresponds to case (B). In contrast to case (A), it is now seen that, on approaching bulk I-A coexistence, the thick film coexists with a zero-layer film (upper curve), while away from bulk coexistence the zero-layer film undergoes a transition directly to a two-layer film (lower curve). This behavior underlies the phase diagram schematically illustrated in Fig. 1(b). In this case, the low value of the zero-layer interfacial tension compared with case (A) can be linked to greater stability of its *partial-drying* state. This in turn can be related to the well-known *contact theorem* [27] which connects the density at the wall to the bulk pressure, and to the fact that, in going from case (A) to (B), the pressure has been significantly reduced due to closer proximity to bulk liquid-vapor coexistence. On the other hand, an explanation for the reduced value of ϵ_w at the wetting transition is due to the *larger* magnitude of ϵ_3^* in this case, compared with case (A). This follows from the fact that part of the "effective" driving forces for orientational ordering at the interface is derived from the ϵ_3 term in the pair potential, as will be discussed further in the next section.

IV. LAYERING MECHANISMS

As was mentioned above in Sec. III C, a *mean-field* theory always predicts a discontinuous translation of the I-A

interface. In other words, a mean-field theory is unable to describe the roughening transition. An intuitive reason for this failure of an *approximate* density-functional model is as follows. Using such a theory, it is possible to calculate the density profile of the I-A interface and the location of the Gibbs dividing surface. This profile corresponds to a local minimum of the appropriate thermodynamic potential which fixes the Gibbs surface at a particular position. However, due to the symmetry of both the smectic and the isotropic phases, a completely equivalent minimum (with the same surface tension) is obtained by simply translating the profile one smectic period. Thus the Gibbs surface will generally move discontinuously from one minimum to another. The only way to allow for continuous movement of the interface is for the latter to be so wide that it is unaffected by the periodicity of the smectic phase. Since the density profile along any direction normal to the interface is always more or less abrupt (i.e., the penetration length is always on the order of the smectic period), a large width of the interface can only be produced by large-scale fluctuations in the position of the interface. While an approximate density-functional theory can properly capture the details of the local density profile, such a theory neglects many-body correlations which are needed to account for these large-scale interface fluctuations.

This argument explains the behavior of layer transitions found in this work at sufficiently large distance from the wall, where the gradient of the wall potential $V_{\rm ex}(z,\theta)$ is small, and forms the basis of our analysis of the infinite-layer transition in Fig. 2. Supporting this view is the fact that we find discrete layering to occur in sufficiently thick smectic films (greater than or equal to 4 layers) adsorbed at the vapor- (V) isotropic interface under state conditions near the bulk V-I-A triple point, in the absence of any wall or external potential [28]. The occurrence of locally stable profiles at this type of interface, differing by a *discrete* number of layers, was not noticed in Ref. [14], and indeed such profiles turn out to be *metastable* relative to those calculated in [14]. Their presence, nonetheless, indicates that the "bulk" mechanism for layer growth at the I-A interface is inherent in a mean-field theory such as is used here. In a more exact calculation, we expect this mechanism to be modified by interfacial roughening fluctuations, as described above. On the other hand, for very thin smectic films, the above "bulk" mechanism is not expected to be appropriate due to a large gradient of the external field near the wall.

In order to better understand the layering mechanism in thin films, we can attempt to analyze the problem in a simplified way, centering our attention only on the developing layer. We assume that the nematic order parameter plays the dominant role in the mechanism of layering, as will be discussed shortly. Therefore we can *hypothetically* integrate out all degrees of freedom except the local nematic order parameter η in a layer. In a more general scheme, coupling between η and other variables (particularly the mean layer density) should also be explicitly considered. Nevertheless, the following analysis remains formally valid for the nematic order parameter or for any other single variable, provided it changes discontinuously at the (first-order) layer transition. After the integration process we would obtain, for the transition in the nth smectic layer, the following single-order-parameter free energy:

$$f(\eta_n) = -TS(\eta_n) - \alpha_n \eta_n^2 - \beta_n \eta_n + O(\eta_n^3), \qquad (6)$$

where η_n is the order parameter of the n^{th} layer, $S(\eta_n)$ is the local orientational entropy, and the remaining terms correspond to the expansion of the interaction energy in powers of the local order parameter. In order to study the nature of the phase transition it is sufficient to retain only the terms explicitly shown in (6). In this case, we have a local Maier-Saupe-type model where the quadratic term $-\alpha_n \eta_n^2$ ($\alpha_n > 0$) is analogous to the standard Maier-Saupe interaction term, and the linear contribution $-\beta_n \eta_n$ ($\beta_n > 0$) is equivalent to that of an external field. The model constructed in this way should be valid to investigate any layer transition, including the "bulk" case. Clearly, however, its utility requires establishing the precise relationships between the coefficients α_n, β_n and the molecular coupling constants ϵ_3, ϵ_3, and ϵ_w, as well as their dependence on T, ρ_b, and layer number n. The general relationships may be very complicated (particularly for the "bulk" case) and we have not attempted to derive them. Instead, we follow simple arguments to obtain the dominant contributions to α_n and β_n for the first layer transition.

Figure 3 shows that the coexisting density and order-parameter profiles for the first few layer transitions differ mainly in the heights of the profile peaks associated with the developing layer. While those profiles indicate that changes in the number density of the layer cannot generally be neglected, the latter effect can be reduced by moving the system further from bulk liquid-vapor coexistence, which reduces the partial-drying nature of the zero-layer surface phase. This is shown in Fig. 8, which

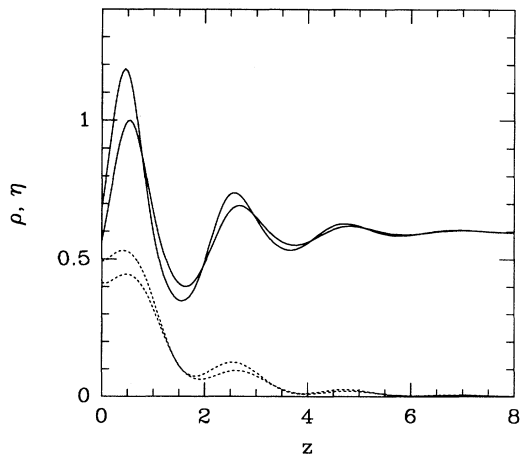

FIG. 8. Coexisting density (continuous lines) and order-parameter (dotted lines) profiles at the 0-1 layer transition for $T = 0.31$ and $\rho_b = 0.6$ and values of the coupling parameters specified in the text.

plots the coexisting profiles at the 0-1 transition at bulk coexistence for the case $T = 0.31$, $\rho_b = 0.6$, $\epsilon_2 = 0.43$, $\epsilon_3 = -0.623\,17$, and $\epsilon_w = 0.3014$. This is similar to case (A), but at a higher bulk density. The main difference from Fig. 3(a) is that now the zero-layer profile also exhibits a substantial density peak near the wall. In this case, it is plausible to view the 0-1 transition as a local *isotropic-nematic* transition in the presence of the external field due to the substrate. In this picture, the main qualitative difference between the two coexisting structures is due to the change in the local orientational order parameter of the layer, rather than in its density. If we neglect changes in the density profile we can consider, for $n = 1$, a simple idealized situation corresponding to a flat density profile with a single narrow peak at the wall. In this case, it can be shown [29] that α_1 will be proportional to ϵ_2 and β_1 will be a linear combination of ϵ_w and ϵ_3. (The dependence on ϵ_3 results from translation-rotation coupling in the pair potential V_A.) Changes in the density profile will renormalize both α_n and β_n. As well, more complicated density profiles may introduce new relationships, such as a dependence of α_n on ϵ_3. However, we believe that even in more general circumstances, the dominant contributions to the parameters α_n and β_n will be those stated here.

As is usual, the local *isotropic-nematic* transition will be driven by competition between the entropy, favoring a free-energy minimum near $\eta_n = 0$, and the Maier-Saupe interaction term $-\alpha_n \eta_n^2$, favoring a minimum at positive η_n when α_n is sufficiently large. For fixed thermodynamic state conditions, and on *neglecting* the external-field term, the transition would occur at a single, unique value of α_n. The value of η_n in the coexisting "nematic" phase would then be given by the Maier-Saupe value, $\eta_{\text{coex}} \approx 0.42$, which supports the "thumb rule" used in Sec. III B for judging the occurrence of a layer transition. The role of the external-field term $-\beta_n \eta_n$ is essentially to stabilize one free-energy minimum against the other. Strictly speaking, as in the "bulk" mechanism (see Sec. III A), the "isotropic" phase in this picture should really be considered a paranematic phase. For a large enough value of β_n, the local nematic-paranematic transition disappears at a critical point [23].

The above picture implies that, under fixed thermodynamic state conditions, the layer transition can only occur for a limited range of values of both α_n and β_n. In particular, if the transition occurs at all, it can only do so for α_n within a finite range of some nonzero value. Due to the presumed dependence of α_n on ϵ_2, this in turn implies that the layer transition disappears both for sufficiently small and sufficiently large values of ϵ_2. We have confirmed this prediction by examining the behavior of the first few layer transitions with changes in ϵ_2. This is illustrated for the 0-1 and 1-2 transitions in Fig. 9, which plots the variation of the discontinuity $\Delta\eta_{\text{int}}$ in the integrated order parameter for these transitions as a function of ϵ_2, at fixed temperature $T = 0.31$ and density of the bulk isotropic phase $\rho_b = 0.6$, as in Fig. 8. In Fig. 9, the wall coupling strength ϵ_w varies as a function of ϵ_2 to maintain coexistence of the different films. The other coupling constant ϵ_3 is also "slaved" to vary

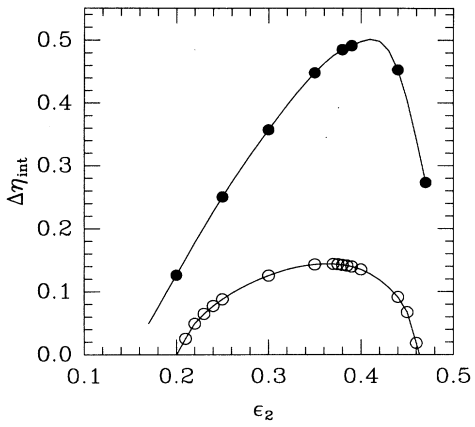

FIG. 9. Discontinuity in η_{int} at the 0-1 (open circles) and 1-2 (filled circles) layer transitions as a function of ϵ_2 for $T = 0.31$ and $\rho_b = 0.6$. The parameters ϵ_w and ϵ_3 vary along with ϵ_2 to maintain both bulk I-A coexistence and the layer transition.

along with ϵ_2 in order to maintain bulk I-A coexistence. The figure shows that $\Delta\eta_{\text{int}}$, which can be considered to measure the strength of the layer transition, exhibits a maximum value and tends toward zero for both large and small values of ϵ_2. In particular, the 0-1 transition completely disappears both for $\epsilon_2 < 0.2$ and $\epsilon_2 > 0.47$, well before reaching the I-N-A triple point which occurs at $\epsilon_2 = 0.555$. A similar behavior is found in the lower density case, $\rho_b = 0.55$ (as shown by Fig. 3 in Ref. [16]), but there the layer transition for large ϵ_2 is preempted by the occurrence of the bulk I-N-A triple point.

These findings can be connected to previous experimental and theoretical results. The key point to note is that increasing or decreasing ϵ_2, with ϵ_3 simultaneously varied to maintain bulk I-A coexistence, corresponds to increasing or decreasing distance from the bulk I-N-A triple point, respectively. [This follows from the nature of the bulk $T - \rho_b$ phase diagram, shown in Fig. 1(b) of Ref. [14], and the feature that the slope of the bulk I-N coexistence curve is essentially proportional to ϵ_2 [29].] The present findings therefore suggest, as a general principle, that smectic layer transitions disappear as the coupling constants are varied to both approach and recede from the bulk I-N-A triple point. This feature is exhibited by the theoretical phase diagram given by Selinger and Nelson [13] (see Fig. 5 in that reference), where it is seen that the 1-2 layer transition in that work occurs only within a narrow range bordering the bulk I-A transition line and disappears both near and far from the bulk I-N-A triple point. These results are also consistent with the finding by Pawlowska *et al.* [12] that there are no discrete-layer transitions at the wall-nematic interface near the first-order bulk N-A transition, despite the fact that the A phase can completely wet that interface.

The above arguments emphasize the qualitative importance of the nematic order parameter to the layering mechanism. In order to obtain layering, it is necessary to have an inhomogeneous density distribution *together* with

a coupling between this inhomogeneity and the nematic order parameter. It is well known that such a coupling is able to change the bulk N-A phase transition from second to first order. A similar mechanism appears to control layering, predicting that layer transitions disappear when the nematic order parameter is saturated either to a large or small value. This is further supported by the finding that our model predicts that layer transitions tend to be smoothed by increasing density, as shown in Fig. 3 of Ref. [16]. Consistent with this is the fact that, for the same parameters as in Fig. 9, the layer transition is completely absent when $\rho_b = 0.7$, a particular example of which is plotted in Fig. 5(c). The feature of a weaker degree of layering with increased density is believed to be an unrealistic outcome of the present theory, resulting from the absence of coupling between anisotropic hard-core interactions (which should dominate at high densities) and the orientational order parameter in our model free energy [14].

Finally, one notes from Fig. 1 and Table I that there is a progressive increase in the values of $\Delta\epsilon_3$ at the layer critical points beyond the 1-2 transition. This indicates increasing dominance by the "bulk" layering mechanism as the smectic film thickens.

V. CONCLUSIONS

Our mean-field calculations have revealed that smectic layering behavior at a semi-infinite substrate surface can be quite rich. We have obtained, for the first time, a full layering-wetting surface phase diagram which reconciles some of the conflicting features predicted by earlier theories [12–14]. We have attempted to explain the variety of surface behavior by two complementary physical mechanisms for layer growth, one based on translation of the bulk I-A dividing surface and the other based on the picture of a local isotropic-nematic transition in the growing layer. While the latter mechanism is strictly applicable only within a narrow range of the model parameters, it is able to provide a clear intuitive picture of the first few layer transitions and, moreover, accounts for earlier theoretical findings that these transitions disappear both sufficiently close to and sufficiently far from the bulk I-N-A triple point. The disappearance on approaching the bulk triple point is consistent with experimental results [3–5], although the latter have not yet been carried out over a sufficiently wide range of homologous liquids to confirm the prediction that layer transitions disappear far away from the triple point.

In this work we have focused on the dependence of surface phase behavior on the molecular coupling constants of the model, rather than on the variation of this behavior with thermodynamic state conditions for *fixed* coupling constants, as might be more appropriate for comparison with experimental results. In addition, the present model utilizes an external substrate potential whose coupling strength is assumed to be independent of the structure of the liquid phase. While appropriate to studies of liquid-solid interfaces [5], this model does not strictly apply to a free interface such as is considered experimentally in Refs. [3,4]. Nonetheless, one might argue similarly to Refs. [12,13] that the free interface should correspond to some suitable "effective" external potential for which the present model is, at least qualitatively, applicable. Our results from studying the effects of the substrate-induced external potential also reveal that a richer variety of behavior than so far detected experimentally may occur, in particular, complete smectic wetting. The absence of this phenomenon in experiments to date suggests that those experiments are confined to the "weak substrate" regime [21]. Variations in the degree of layerwise smectic growth under different surface treatments, recently observed in studies of 12CB confined within porous membranes [6], indeed hint at the possibility of finding complete smectic wetting.

We shall close with some remarks on the limitations of the present work and on other aspects of smectic layering yet to be resolved. As already noted, the theory does not adequately take account of orientational coupling due to anisotropic hard-core interactions, which predicts the loss of layering with increasing liquid density. This may also be responsible for the fact that we are unable to generate stable discrete-layer states at a true liquid-vapor interface [14]. The other principal limitation is due to the neglect of fluctuations, both elastic fluctuations in the bulk smectic phase (which destroy true long-range order in that phase) and roughening fluctuations at the I-A interface. As also noted earlier, the latter fluctuations will likely destroy the infinite number of layer transitions in the case of complete smectic wetting, but may still leave in place a single prewetting transition such as that found here, albeit unaccompanied by discrete layering in the thick-film region [21]. An earlier study [25] predicted that elastic correlations in a smectic film may destroy smectic wetting altogether, while simultaneously *enhancing* the number of layer transitions in the partial-wetting region due to coupling between elastic and interfacial fluctuations: see also Ref. [13]. It is at present difficult to incorporate these fluctuations in a molecular theory of the type used here, and clearly further work on understanding these effects is desirable.

More recent experimental studies with finer resolution, at both solid-liquid [5] and free [30] interfaces, have concluded that the layer transitions in pure 12CB are second order, although they may be driven first order by addition of impurities. These results have been connected [30] to the presence of a tricritical point on each layer-transition line, although here we have found that such a point occurs only for the infinite-layer transition, where it is a purely bulk effect. An alternative explanation, more consistent with present theory (and also suggested in Ref. [30]) is that such apparent "second-order" transitions are *not* true transitions but represent pretransitional anomalies similar to that shown in Fig. 5(c). Again, further studies to resolve this question are called for.

ACKNOWLEDGMENTS

A.M.S. and L.M. acknowledge support from Grant No. PB91-0090 of DGCyT (Spain). D.E.S acknowledges financial support from NSERC (Canada).

[1] T. J. Sluckin and A. Poniewierski, in *Fluid Interfacial Phenomena*, edited by C. A. Croxton (Wiley, New York, 1986), p. 215.
[2] B. Jerome, Rep. Prog. Phys. **54**, 391 (1991).
[3] B. M. Ocko, A. Braslau, P. S. Pershan, J. Als-Nielsen, and M. Deutsch, Phys. Rev. Lett. **57**, 94 (1986).
[4] P. S. Pershan, Faraday Discuss. Chem. Soc. **89**, 231 (1990).
[5] B. M. Ocko, Phys. Rev. Lett. **64**, 2160 (1990).
[6] G. S. Iannacchione, J. T. Mang, S. Kumar, and D. Finotello, Phys. Rev. Lett. **73**, 2708 (1994).
[7] J. Xue, C. S. Jung, and M. W. Kim, Phys. Rev. Lett. **69**, 474 (1992).
[8] B. Rapp and H. Gruler, Phys. Rev. A **42**, 2215 (1990).
[9] T. Stoebe, P. Mach, and C. C. Huang, Phys. Rev. Lett. **73**, 1384 (1994).
[10] M. G. J. Gannon and T. E. Faber, Philos. Mag. A **37**, 117 (1978).
[11] D. Beaglehole, Mol. Cryst. Liq. Cryst. **89**, 319 (1982).
[12] Z. Pawlowska, T. J. Sluckin, and G. F. Kventsel, Phys. Rev. A **38**, 5342 (1988).
[13] J. V. Selinger and D. R. Nelson, Phys. Rev. A **37**, 1736 (1988).
[14] L. Mederos and D. E. Sullivan, Phys. Rev. A **46**, 7700 (1992).
[15] W. L. McMillan, Phys. Rev. A **4**, 1238 (1971).
[16] A. M. Somoza, L. Mederos, and D. E. Sullivan, Phys. Rev. Lett. **72**, 3674 (1994).
[17] D. E. Sullivan and M. M. Telo da Gama, in *Fluid Interfacial Phenomena*, edited by C. A. Croxton (Wiley, Chichester, 1986), p. 45; S. Dietrich, in *Phase Transitions and Critical Phenomena*, edited by C. Domb and J. Lebowitz (Academic Press, London, 1988), Vol. 12.
[18] L. Mederos and D. E. Sullivan, Phys. Rev. A **39**, 854 (1989).
[19] W. Maier and A. Saupe, Z. Naturforsch. Teil A **13**, 564 (1958).
[20] P. Tarazona, U. Marini Bettello Marconi, and R. Evans, Mol. Phys. **60**, 573 (1987).
[21] R. Pandit, M. Schick, and M. Wortis, Phys. Rev. B **26**, 5112 (1982).
[22] E. H. Hauge and M. Schick, Phys. Rev. B **27**, 4288 (1983).
[23] P. J. Wojtowicz and P. Sheng, Phys. Lett. **48A**, 235 (1974).
[24] I. Lelidis and G. Durand, Phys. Rev. Lett. **73**, 672 (1994).
[25] L. V. Mikheev, Zh. Eksp. Teor. Fiz. **96**, 632 (1989) [Sov. Phys. JETP **69**, 358 (1989)].
[26] D. A. Huse, Phys. Rev. B **30**, 1371 (1984).
[27] J. P. Hansen and I. R. McDonald, *Theory of Simple Liquids* (Academic, New York, 1986).
[28] Y. Martinez, A. M. Somoza, L. Mederos, and D. E. Sullivan (unpublished).
[29] B. Tjipto-Margo and D. E. Sullivan, J. Chem. Phys. **88**, 6620 (1988).
[30] G. J. Kellogg, P. S. Pershan, E. H. Kawamoto, W. F. Foster, M. Deutsch, and B. M. Ocko, Phys. Rev. E **51**, 4709 (1995).